

# Investigation of hydroxyapatite-titanium composite properties during heat treatment

AXAULE MAMAEVA<sup>1</sup>, AIDAR KENZHEGULOV<sup>1, 2, 4</sup>,  
PIOTR KOWALEWSKI<sup>3\*</sup>, WOJCIECH WIELEBA<sup>3</sup>

<sup>1</sup> Institute of Metallurgy and Ore Beneficiation, Joint-stock company, Almaty, Republic of Kazakhstan.

<sup>2</sup> Institute of Combustion Problems, Almaty, Republic of Kazakhstan.

<sup>3</sup> Faculty of Mechanical Engineering, Wrocław University of Science and Technology, Wrocław, Poland.

<sup>4</sup> Kazakh National Research Technical University, Almaty, Republic of Kazakhstan.

A biocompatible hydroxyapatite (HA) coating with a thickness of about 18–20 microns was successfully deposited by radio-frequency (RF) magnetron sputtering on titanium substrates VT1-0. The data obtained for the optimal composition and structure of hydroxyapatite can be used to create coating which will interact with a titanium substrate. Using the methods of optical and SEM, AFM, electron microprobe, FTIR and X-ray analysis, surface morphology, phase and elemental composition, structure of hydroxyapatite (HA) coatings were studied. Structural and phase transformations after heat treatment using X-ray diffraction and microscopic methods of analysis were studied. It was found that after annealing coating phase analysis showed the presence of not only hydroxyapatite ( $\text{Ca}_5(\text{PO}_4)_3\text{OH}$ ), but also compounds of tricalcium phosphate ( $\text{Ca}_3(\text{PO}_4)_2$ ) and titanium oxide. Adhesive-tribological durability, friction and deformation characteristics of hydroxyapatite coating on titanium substrate were determined. The obtained coatings had high hardness, wear resistance and adhesion to the substrate and low modulus of elasticity and coefficient of friction.

*Key words:* hydroxyapatite (HA), titanium, magnetron sputtering, heat treatment, composite

## 1. Introduction

Biomaterials are used for manufacturing of devices intended to replace a functional body part in a safe, reliable, economical, and physiologically acceptable form. At the present, a variety of devices and materials used in the treatment of diseases or injuries include such familiar names as sutures, needles, catheters, plates for connecting bone fragments, tooth fillings, etc. [16].

Titanium and its alloys are widely used for production of bone and dental implants [16]. This is the result of their high biocompatibility (corrosion resistance) and mechanical properties, especially low elastic modulus, which reduce stress shielding. The mechanical properties of implant material are the most

important in the contact with degraded bone tissue, like in the case of osteoarthritis disease [22]. However, metal implants could cause infections which are the common clinical complications [10]. Also, the tribological properties of titanium alloys endoprostheses (size of PE-UHMW wear debris) are not as good as the others metallic biomaterials. Those negative effects could be reduced by application of diverse kinds of coatings. The nitrogen implantation [23], ultrapassivation of titanium and thermal oxidation [1] have become a standard procedure for improving a titanium alloys surface [9].

To increase the biocompatibility of titanium alloys in orthopedic applications hydroxyapatite (HA) coatings are widely used. HA has an excellent biocompatibility and adhesion to living tissue. For example, a naturally carbonated hydroxyapatite is main compo-

\* Corresponding author: Piotr Kowalewski, Faculty of Mechanical Engineering, Wrocław University of Science and Technology, ul. Ignacego Łukasiewicza 7/9, 50-371 Wrocław, Poland. Phone: +48 506 47 35 53, E-mail: piotr.kowalewski@pwr.edu.pl

Received: December 6th, 2016

Accepted for publication: April 7th, 2017

ment of arterial calcium deposits [21]. However, hydroxyapatite possesses poor mechanical properties (hardness) and only tolerate limited loads for implants. Since hydroxyapatite has excellent biocompatibility, it is brittle and easier to break down than human body bone [4], [19]. Titanium is a well-known material applied in implant that has advantage in mechanical properties [15] but is poor as far as biocompatibility is concerned [6]. The combination of the titanium alloy and HA is expected to produce bioimplants with good mechanical properties and biocompatibility [2], [20]. Hydroxyapatite is not only a biocompatible, osteoconductive, non-toxic, noninflammatory and nonimmunogenic agent, but it has the ability to form a direct chemical bond with living tissues [14].

The problem of biocompatibility of materials is very relevant in the medical materials science and engineering of biological tissues [3]. The properties of implant's surface play a special role in the integration of the implant with living tissues [13], with electrical compatibility at all levels of biological organization of living systems (molecular, cellular, tissue) as one of the most important characteristics.

By virtue of the fact that almost all the interactions between cells and tissues with a biological material at the "tissue-implant" interface refer to surface phenomena, surface properties of the implant material, such as mechanical clutch, as a result of the germination of tissue in the implant structure, chemical tissue interaction with the components of the elemental composition of the implant [24] are important.

There are many different methods to fabricate the HA coating on implant surface in the field of biomedical applications. The commonly known are: physical vapor deposition (PVD), plasma treatments (APP) [7], cold gas dynamic spraying deposition [10] and powder metallurgy [2].

The main purpose of the present experiment was to analyze mechanical properties and interactions between HA and Ti alloy under various sintering temperatures.

## 2. Materials and methods

The upgraded installation VUP 5M with magnetron source was used for deposition of calcium – phosphate coatings. The operating frequency of RF generator is 5.28 MHz. The following sputtering modes of coatings were used: the argon pressure of

argon of 0.1 Pa (ultimate pressure in the vacuum chamber of  $10^{-4}$  Pa), the distance between the target and substrate of 40 mm.

In this paper, titanium VT1-0 substrates (chemical composition Fe – 0.25, Si – 0.1, Ti – 99.7, O – 0.2) with the purity of 99.5% (Nilaco Corporation, Japan) were chosen. Before sputtering, all samples were mechanically grinded and polished as the completeness of the treatment depends on the strength of the coating adhesion to the work piece and the quality of the coating. Next, after polishing a chemical etching of samples in a solution of 1 mL HF + 2 mL HNO<sub>3</sub> + 2.5 mL H<sub>2</sub>O was performed. The target was a hydroxyapatite powder with dispersion <63 microns.

At the first stage, the synthesized (with coating) samples were annealed in vacuum of  $10^{-3}$  Pa, at temperatures ranging from 600 °C to 1100 °C for 1 hour, followed by cooling in furnace.

X-ray diffraction analysis was carried out on D8 Advance (BRUKER), equipment with radiation of  $\alpha$ -Cu. Work mode of D8 Advance (BRUKER) installation: CuK $\alpha$  – radiation ( $\lambda \approx 1,54$  Å);  $U = 40$  kV,  $I = 40$  mA; angle range  $2\Theta$  4–90° to scan step 0,01°. For phase analysis database PDF 2 was used.

Transmission electron microscopy TEM was performed on a JEOL CX at accelerating voltage of 100 kV. TEM samples were prepared on a carbon substrate with a net coating.

The study of surface morphology was performed by scanning electron microscopy using microscope JXA-8230 (JEOL) at accelerating voltage of 20 kV and a current of the electron beam of 7 nA. The back-scattered electron mode (COMP) was used for all sections of the samples chosen for scanning electron microscopic (SEM) study.

The adhesive – tribological tests to determine the mechanical and tribological properties were carried out on a scratch tester REVETEST (CSM Instruments) with optical microscope and scanning electron microscope Quanta 200 3D.

All these methods have been used to examine the coating's surface morphology, phase composition, mechanical and tribological properties after heat treatment.

## 3. Results

The radiographs in Fig. 1 show the influence of mechanical treatment on the titanium substrate. After machining, the peak (002) which is the most clear in

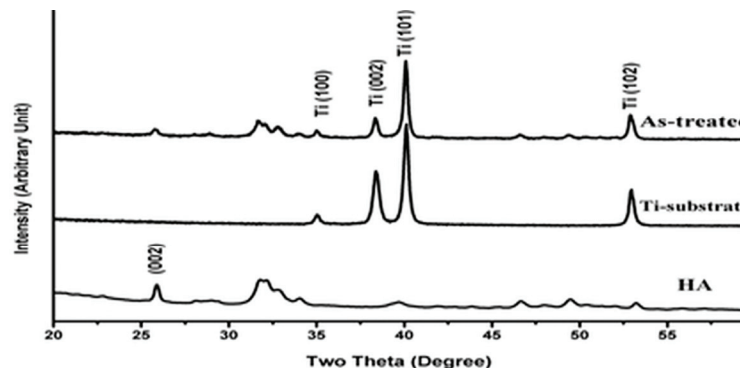


Fig. 1. X-ray diffraction of HA, Ti substrate and HA coating on a titanium substrate

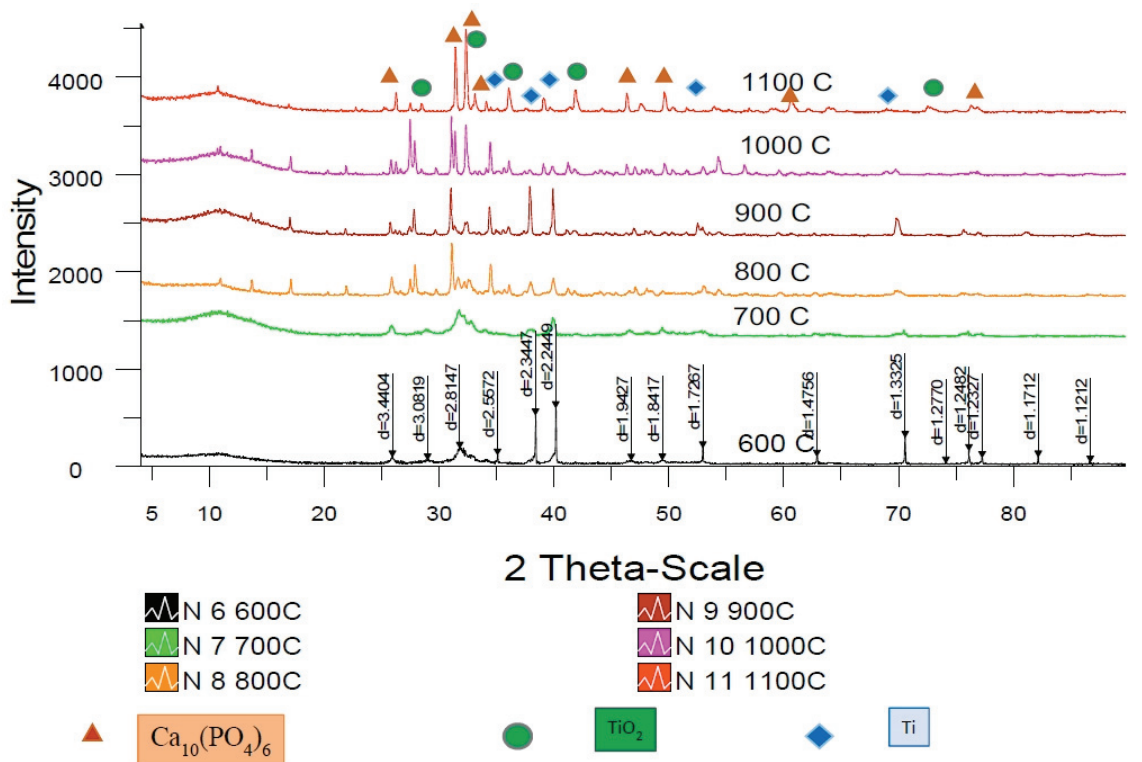


Fig. 2. Radiographs of deposited HA after annealing

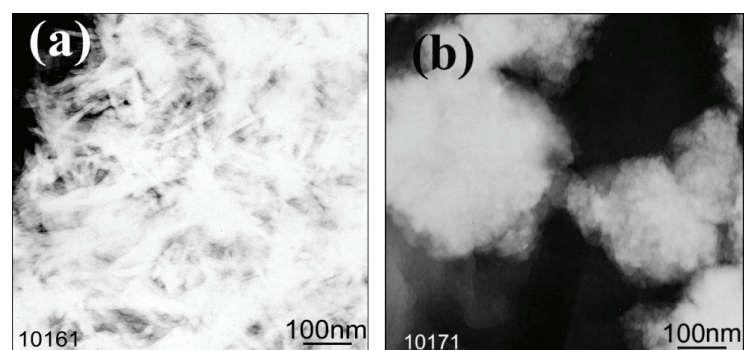


Fig. 3. TEM images of mechanically crushed HA samples

the radiograph for HA shows a significant decrease in the intensity. The peak (101) of titanium substrate slowly shifts to higher values rising from level  $\Delta d = 0,0024$  to  $\Delta d = 0,0015$  and  $\Delta d = 0,0016$  for (002) and (102), respectively.

X-ray results of deposited HA after annealing at different temperatures are shown in Fig. 2.

TEM images of HA show crystallites of not only a needle, but also a rounded shape that illustrates agglomeration of the particles (Fig. 3).

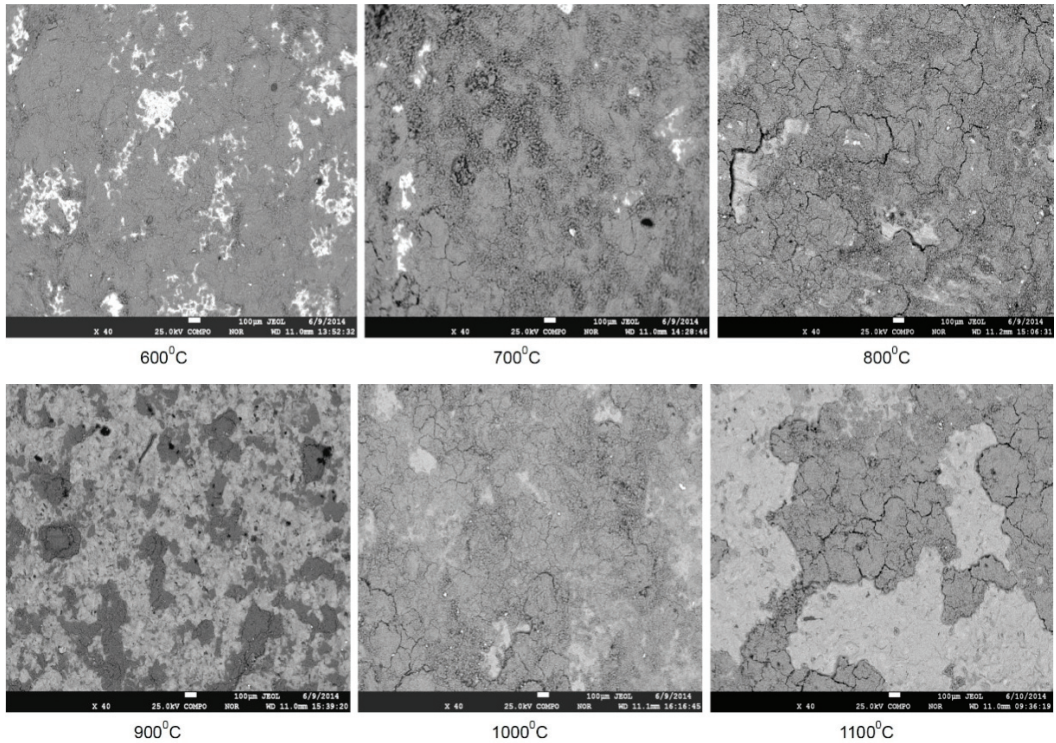


Fig. 4. The surface of the titanium sample after annealing for an hour

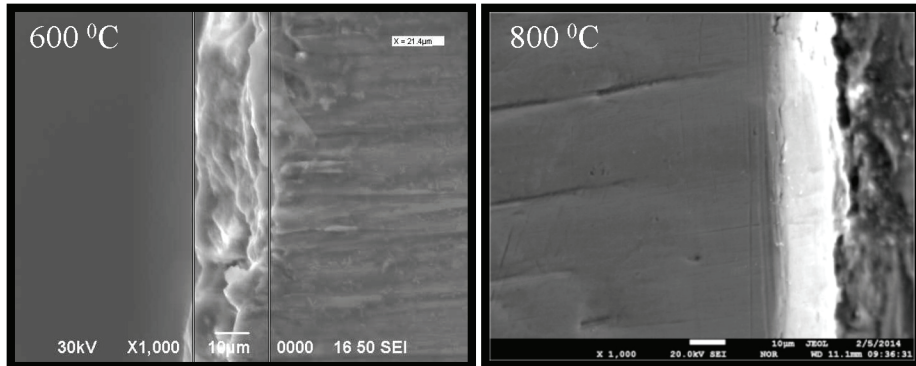


Fig. 5. Cross-section of HA coatings on titanium substrate

Investigation of the influence of heat treatment on the morphology of the biocomposite during investigation have also been done.

Figure 4 shows a typical SEM surface morphology of the coated substrate after annealing for 1 hour in the temperature range from 600 to 1100 °C.

Typical cross-sections of deposited HA coatings on a cross section of samples on SEM are shown in Fig. 5, the coating thickness of the sample treated at 600 °C is about 21.4 microns. The coating layer dissociated at the temperature higher than 800 °C.

The composition of the sample coated with HA was analyzed using energy dispersive X-ray spectroscopy. Energy dispersive spectroscopy of the deposited sample, a number of spot tests found that the average

value of Ca/P of HA coating ratio was  $(1.803 \pm 0.18)$  while the ideal molar ratio in a stoichiometric HA is  $(1.67)$  [8].

As a result of significant plastic deformation during the thermal influence, along with the indicated change of mechanical properties, the microstructure of Ti substantially improves. It is noted that thermal treatment leads to selective measures of increased micro hardness of the surface (Fig. 6). The elastic modulus (Young's modulus)  $E$  is associated with Vickers micro hardness with equation.  $E$  and  $Y$  values have been calculated for a load of 200 g using the above given equations and shown in Table 1. The values of the yield strength of conventional titanium alloys are in the range between 800 and 1200 MPa

(81.6 and 122.4 kg/mm<sup>2</sup>) with the highest values exhibited by metastable  $\beta$ -alloys [17].

The transition from phase  $\alpha$  to  $\beta$  is accompanied by the increase of micro-hardness up to 900 °C. Further measurement of these changes is not possible, because the sample surface gets dark due to high temperature and patterns on printouts prints are not extinguishable.

To determine the mechanical and tribological properties, adhesive – tribological tests were carried out on a scratch tester REVETEST (CSM Instruments) with optical microscope and scanning electron microscope Quanta 200 3D.

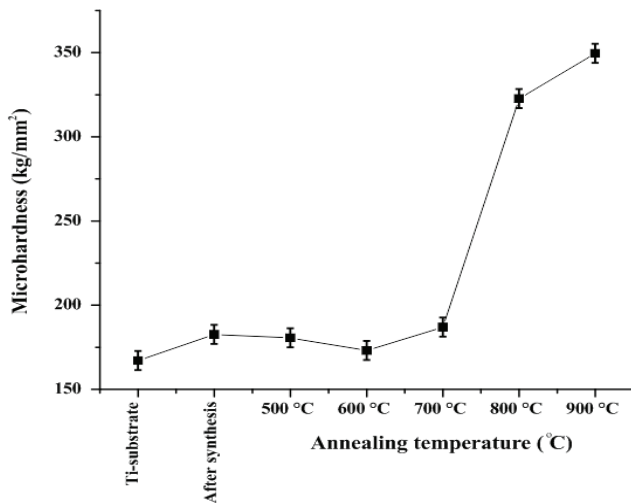


Fig. 6. Changes of micro hardness of titanium substrate after annealing

Table 1. Average values of  $H_v$ ,  $E$  and  $Y$  for titanium substrate depending on temperature

Temperature	Vickers micro hardness $H_v$ (kg/mm <sup>2</sup> )	Young's modulus $E$ (kg/mm <sup>2</sup> )	Yield strength, $Y$ (kg/mm <sup>2</sup> )
Ti-substrate	167	13698.5	55.7
After synthesis	182.6	14967.6	60.9
500 °C	180.6	14808	60.2
600 °C	173.1	14187.2	57.7
700 °C	186.9	15324.6	62.3
800 °C	322.7	26455.8	108
900 °C	349.5	28645.1	117

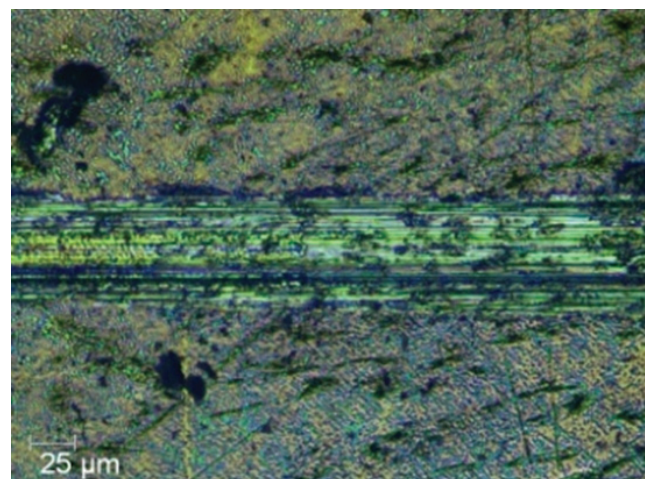


Fig. 7. The surface of the sample after tribological tests for sample HA/titanium annealed at a temperature of 600 °C

Adhesive – tribological tests were carried out under the following conditions: the load on the indenter

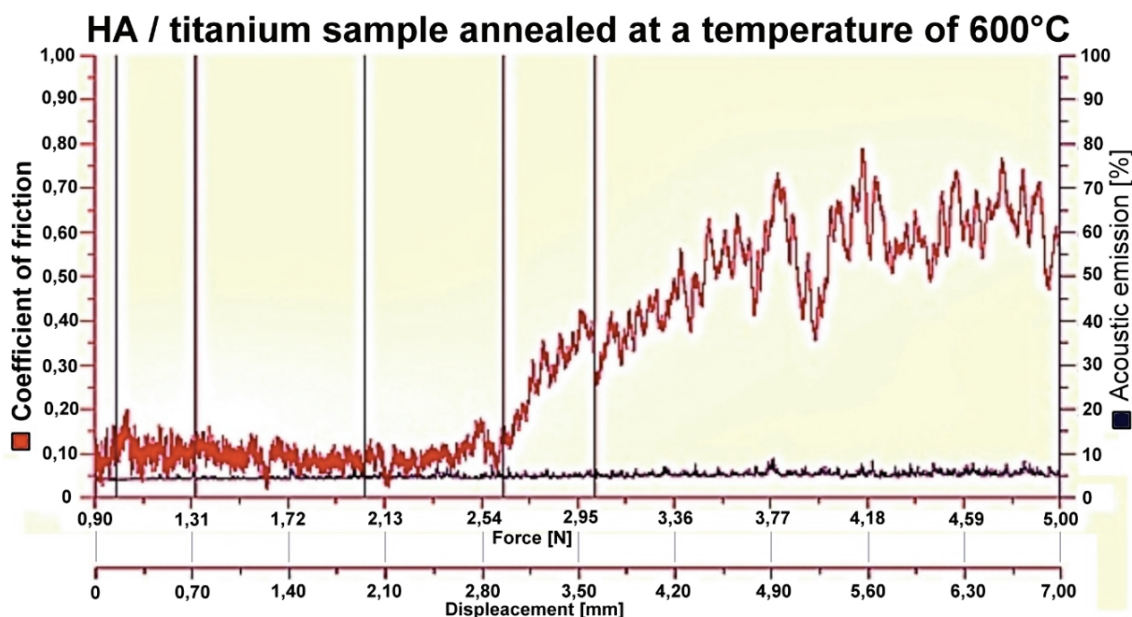
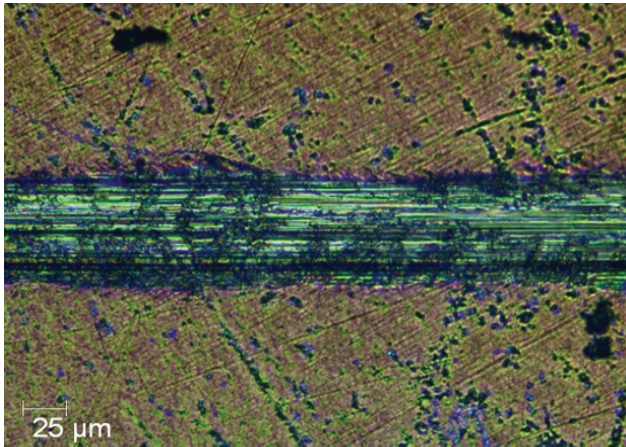


Fig. 8. Plot of friction for sample HA/titanium annealed at a temperature of 600 °C

was growing from 0.9 to 5N, speed of moving of the indenter was 1mm/min, the length of the crack was 7 mm, the loading rate was 0.59 N/m and the frequency of digital signal – 60, acoustic emission – 9. The environmental conditions were: temperature of 20 °C and relative humidity of 55%. The normal force, the COF and acoustic emission were obtained by REVETEST CSM tester with diamond tip.



At first, on Figures 7 and 8, an optical image of sample's surface after tribological tests and plot of friction for sample HA/titanium annealed at a temperature of 600 °C can be seen.

The coefficient of friction for the sample with HA coating annealed at 800 °C initially was equal to 0.25 (Fig. 9). After burnishing, the friction coefficient increased to 0.28 (Fig. 10).

Fig. 9. The surface of the sample after tribological tests for sample HA/titanium annealed at a temperature of 800 °C

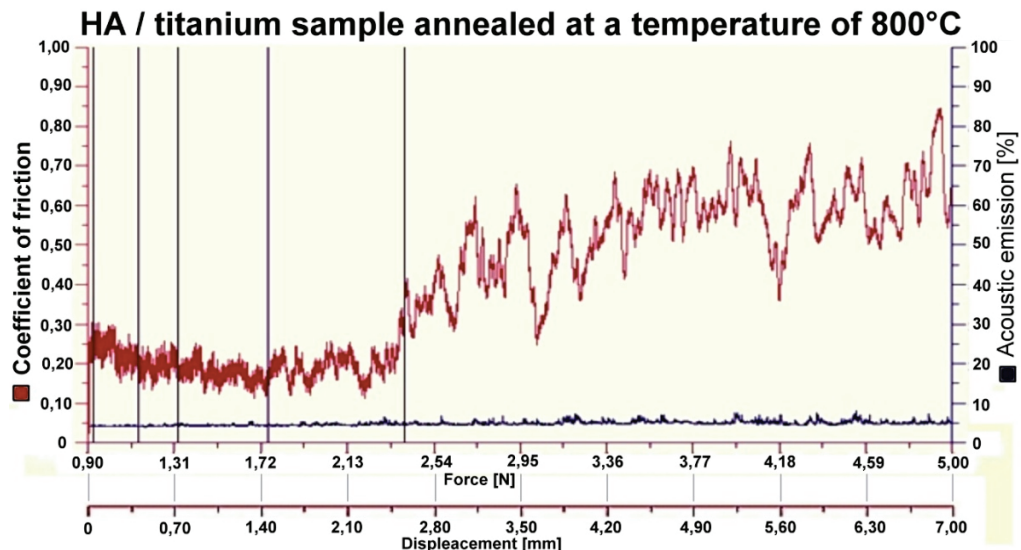


Fig. 10. Plot of friction for sample HA/titanium annealed at a temperature of 800 °C

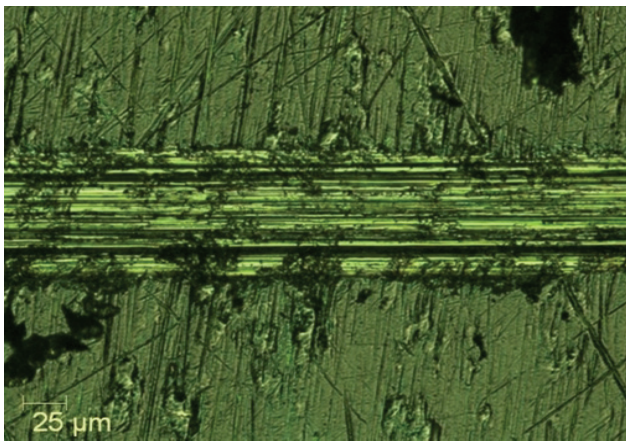


Fig. 11. Surface abrasion under high loads for the sample HA/Ti annealed at a temperature of 900 °C

The results of COF and acoustic emission have been shown in Fig. 12. HA coating annealed at 900 °C. The values of friction coefficient are slightly smaller (avg. 0,03) than for HA coating annealed at 800 °C (Fig. 10) but still much higher than for coating made in 600 °C (Fig. 8).

samples. The X-ray peaks of the formed phases were coordinated with standard ICDD (JCPDS),  $\alpha$ -tricalcium phosphate (09-0348),  $\beta$ -tricalcium phosphate (03-0690) and titanium oxide (29-1361). Radiograph of the treated sample shows that after treatment HA exhibits broader peaks, which may be caused due to very small crys-

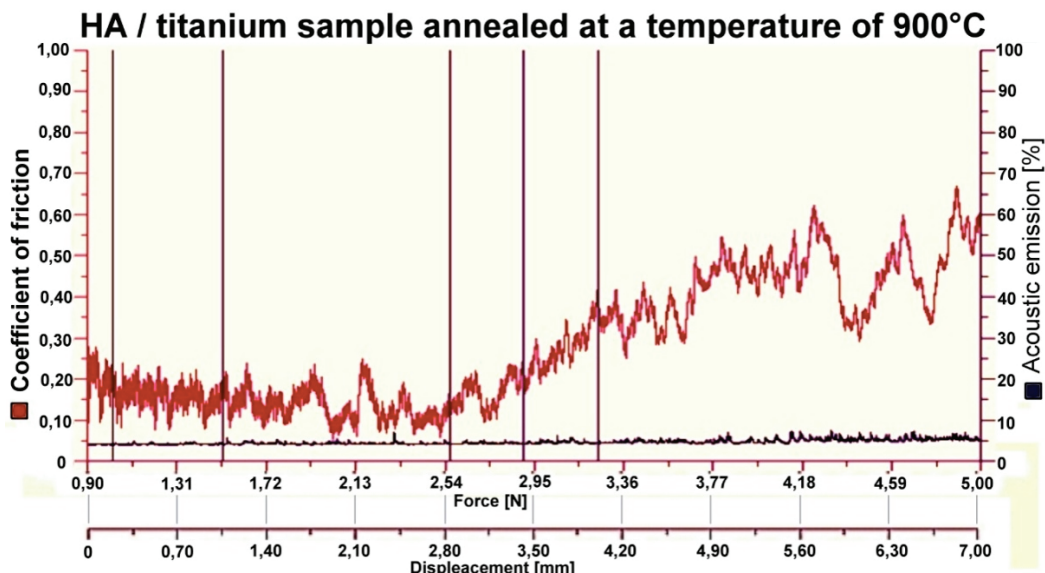


Fig. 12. Plot of friction for sample HA/titanium annealed at a temperature of 900 °C

Surface abrasion under high loads for the sample HA/titanium annealed at a temperature of 900 °C is shown in Fig. 11.

## 4. Discussion

After analysis of the radiographs (Fig. 1) accordingly to [18], the process of coating of HA metal surfaces at elevated temperatures (plasma deposition) tends to exclude-OH functional groups in the matrix of HA (dehydration) and leads to degradation of HA to  $\alpha$ -tricalcium phosphate,  $\beta$ -tricalcium phosphate and tetracalcium phosphate. High temperatures of the substrate contributed to oxidation of the substrate surface prior to the growth of HA layer. The oxide layer deteriorated adhesion of the coating and the substrate. Therefore, HA crystalline coatings should be precipitated at lower temperatures to obtain coatings with greater adhesion [5]. As shown in their radiographs (X-ray diffraction), repeated collision of balls with the substrate results in the deposition of the HA powder on their surface at a temperature close to room temperature without subsequent expansion of HA (Fig. 1).

Changes in radiographs (Fig. 2) indicate the effect of temperature on stability of the structure of the sam-

tallite size of HA. In accordance with radiographs of coated samples, it is evident that up to 700 °C samples of HA did not show any signs of decomposition or phase transitions. The increase in annealing temperature results in the increase of in the peak intensity of HA compared to the sample annealed at a temperature of 600 °C. With the increase of thermal impact up to 800 °C radiographs begin to indicate a slight decomposition of HA to  $\text{Ca}_3(\text{PO}_4)_2$ .

The TEM investigations of the HA coating demonstrated that crystallites of HA have not only a needle structure, but also rounded shapes (Fig. 3).

The presence of cracks at the temperatures of 700 to 1100 °C may be caused by the difference in thermal coefficients of expansion of HA and titanium alloy substrate. Mahe M. et al. [11] reported formation of cracks during the sintering of ceramic films for cases of differential sintering, resulting in a voltage incompatibility. During sintering the cracks develop to greater extent from the intrinsic defects. As a result, problems of cracking and decohesion can also develop during cooling of annealed ceramic films deposited on the substrate due to the difference of the temperature expansion coefficients of the substrate and the deposited film. The overall results show heat treatment of more than 800 °C leads to the formation of cracks and the degradation of the film.

In the case of cross section SEM image in Fig. 5, left image indicated HA-deposited coating after annealing at a temperature of 600 °C. It was found that coating was without cracks and had thickness of 21.4 microns. Along with increasing annealing temperature the coating undergoes some changes and degradation of the film begins after 800 °C (Fig. 5). The results indicate, on the whole, that coating's surface morphology after annealing with increasing temperature leads to changes such as wrinkles and other degradation of the film.

According to micro-hardness results, it can be noticed that heat treatment of titanium samples up to 600 °C is accompanied by a slight decrease in micro hardness (Fig. 6). With increasing temperature, the micro hardness increases dramatically due to the phase transition of the titanium substrate from phase  $\alpha$  to  $\beta$ .

The application of the international standards to the measurements of practical adhesion of biocompatible nano- and micro-thin films by scratch testers offers great advantages in research area because it is a very simple way of measuring and evaluating the properties of thin layers. The authors [12] designed and verified the standardized conditions and procedures for measuring practical adhesion of film whose thickness ranges from 0.10 to 20  $\mu\text{m}$ . This range of thickness is typical of biocompatible nano- and micro-thin films as in this case the thickness of the coatings is 18–21.4 microns.

Analysis of measurement data on the friction force of the indenter for the sample with HA coating annealed at a temperature of 600 °C showed (Fig. 7) decrease of frictional forces in the range of normal load  $F_n$  on average to 30% for the coating. The friction coefficient of the sample at the initial stage is 0.12. Apparently, this is the lowest value (Fig. 8) because of the very small roughness of almost smooth coating.

At the stage of running in, friction coefficient increases to 0.20, due to the increase of load, and then at the stage of steady wear it is 0.12. At the next stage, after the friction of 2.50 mm, a gradual destruction of the coating, i.e., abrasive wear takes place (there are several potholes). The friction coefficient increases to 0.60 (not very high hardness of the coating). Reduction of friction coefficient to 0.15 at the stage of the running in is due to the low roughness of the coating, and then at the stage of steady wear it is 0.20, which gives us the possibility to state that it is not hard coating. At the next stage, after 2.70 mm of the passed distance, there takes place a gradual destruction of the coating; there form a few chips along the border of the impact of the indenter are performed (abrasive wear). The coefficient of friction increases up to 0.55.

Due to the high roughness of the coating, the value of the steady depreciation is equal to 0.10, which gives

us the opportunity to state that it is the hardest coating. At the next stage, after the friction of 2.10 mm, the coating is destructed (there are potholes, cracks) – abrasion. The coefficient of friction increases up to 0.85. The destruction of the coating begins with the appearance of individual chevron cracks at the bottom of the groove of wear resulting in the increase of local stresses and friction.

Calcium-depleted HA is thermally less stable than the stoichiometric HA. It is believed that the increase in the diffusion coefficient is caused by the introduction of structural defects such as grain boundaries and interfaces. The correlation between an increased diffusion coefficient and microstructure of the composite often affects the increase in reaction temperature with a simultaneous improvement of the microstructure of composite.

It should be noted that the increase in the load curve describing the dependence of the friction coefficient on the load has a oscillatory nature: the increase in the coefficient of friction is accompanied by a sharp burst of acoustic emissions and slowing down of the penetration of the indenter from 0 to 67  $\mu\text{m}$  deep into the material (Fig. 11). Such behavior of all recorded parameters indicates that the soft coating with the thickness greater than 1 micron on the surface of a hard material provides substantial resistance to diamond indenter up to its complete abrasion under high loads (Fig. 12).

Thus, adhesion and tribological tests have allowed determining the adhesive strength, friction and deformation characteristics of the hydroxyapatite coating on titanium substrate. The process of elastic and plastic deformation in the system coating/substrate were evaluated and threshold values of the critical load were determined based on the measurement of various physical parameters in the process of adhesion tests. The coatings had high hardness, wear resistance and adhesion to the substrate and low modulus of elasticity and coefficient of friction.

## 5. Conclusions

The results of the study and discussion enable formulation of the following conclusions. In the course of the present study hydroxyapatite coatings with a thickness of about 18–21.4 microns on the substrate of titanium alloy were obtained. The increase the temperature of thermal annealing resulted in development of small cracks on the surface and phase analysis shows the presence of not only hydroxyapatite –  $\text{Ca}_5(\text{PO}_4)_3\text{OH}$  but also compounds of tricalcium phosphate  $\text{Ca}_3(\text{PO}_4)_2$  and

titanium oxide. Adhesive-tribological durability, friction and deformation characteristics of hydroxyapatite coating on titanium substrate were determined. The obtained coatings had high hardness, wear resistance and adhesion to the substrate and low modulus of elasticity and coefficient of friction.

## References

- [1] ANIOLEK K., KUPKA M., BARYLSKI A., *Sliding wear resistance of oxide layers formed on a titanium surface during thermal oxidation*, J. Wear, 2016, 356–357, 23–27.
- [2] ARIFIN A., SULONG A.B., MUHAMAD N., SYARIF J., *Characterization of hydroxyapatite/Ti6Al4V composite powder under various sintering temperature*, Teknologi, 2015, 75(7), <http://dx.doi.org/10.11113/jt.v75.5168>.
- [3] BANASZEK K., WIKTOROWSKA-OWCZAREK A., KOWALCZYK E., KLIMEK L., *Possibilities of applying Ti (C, N) coatings on prosthetic elements – research with the use of human endothelial cells*, Acta of Bioengineering and Biomechanics, 2016, 18(1), 129–136.
- [4] JANICKI T., SOBCZAK-KUPIEC A., SKOMRO P., WZOREK Z., *Surface of root cementum following air-polishing with bioactive hydroxyapatite (Ca and P mapping). A pilot study*, Acta Bioeng. Biomech., 2012, 14.1, 31–8.
- [5] KATTO M., ISHIBASHI K., KUROSAWA K., YOKOTANI A., KUBODERA S., KAMEYAMA A., HIGASHIGUCHI T., NAKAYAMA T., KATAYAMA H., TSUKAMOTO M., ABE N., *Crystallized hydroxyapatite coatings deposited by PLD with targets of different densities*, J. Journal of Physics, 2007, 59, 75–78.
- [6] KIEL-JAMROZIK M., SZEWCZENKO J., BASIAGA M., NOWIŃSKA K., *Technological capabilities of surface layers formation on implant made of Ti-6Al-4V ELI alloy*, Acta Bioeng. Biomech., 2015, 17(1), 31–37.
- [7] KOT M., KOBIELARZ M., MAKSYMOWICZ K., *Assessment of mechanical properties of arterial calcium deposition*, J. Transactions of FAMENA, 2011, 35(3), 49–56.
- [8] LEE H.J., KWON T.Y., KIM K.H., KANG S.S., CHOI S.H., KWON S.T., CHO D.H., SON J.S., *In vitro evaluation of hydroxyapatite-coated titanium implant with atmospheric plasma treatment*, J. Journal of Nanoscience and Nanotechnology, 2015, 15(8), 5593–5596.
- [9] LEYENS C., PETERS M., *Titanium and Titanium alloys*, Wiley-VCH Verlag GmbH & co., KGaA, 2003.
- [10] MOHSENI E., ZALNEZHAD E., BUSHROA A.R., HAMOUDA A.M., GOH B.T., YOON G.H., *Ti/TiN/Ha coating on Ti-6Al-4V for biomedical applications*, J. Ceramics International, 2015, 41(10), 14447–14457.
- [11] MAHE M., HEINTZ J., RODEL J., REYNERS P., *Cracking of titania nanocrystalline coatings*, J. Journal of the European Ceramic Society, 2008, 28, 2003–2010.
- [12] PATRIK K., JAN M., *The procedure of evaluating the practical adhesion strength of new biocompatible nano- and micro-thin films in accordance with international standards*, Acta Bioeng. Biomech., 2011, 13(3), 87–94.
- [13] SANPO N., THARAJAK J., *Biocompatibility of cold sprayed silver-doped hydroxyapatite/titanium coatings*, J. Applied Mechanics and Materials, 2016, 848, 19–22.
- [14] SOBCZAK A., KOWALSKI Z., WZOREK Z., *Preparation of hydroxyapatite from animal bones*, Acta Bioeng. Biomech., 2009, 11.4, 23–28.
- [15] SOKOŁOWSKI G., RYLSKA D., SOKOŁOWSKI J., *The effect of heat treatment simulating porcelain firing processes on titanium corrosion resistance*, Acta Bioeng. Biomech., 2016, 18(2), 93–102.
- [16] SUN L., BERNDT C.C., GROSS K.A., KUCUK A., *Material fundamentals and clinical performance of plasma sprayed hydroxyapatite coatings*, J. Biom. Mater. Res., 2001, 58, 570–592.
- [17] TAO N.R., LU J., LU K., *Surface nanocrystallization by surface mechanical attrition treatment*, J. Materials Science Forum, 2008, 579, 91–108.
- [18] TOMANIK M., NIKODEM A., FILIPIAK J., *Microhardness of human cancellous bone tissue in progressive hip osteoarthritis*, Journal of the Mechanical Behavior of Biomedical Materials, 2016, 64, 86–93.
- [19] WEN J., LI Y., ZUO Y. et al., *Preparation and characterization of nano-hydroxyapatite/silicone rubber composite*, J. Mater. Lett., 2008, 62, 3307–3309.
- [20] WOJAK I., SCHARNWEBER D., PAMUŁA E., *Resorbable scaffolds modified with collagen type I or hydroxyapatite: in vitro studies on human mesenchymal stem cells*, Acta Bioeng. Biomech., 2013, 15.1, 61–67.
- [21] YODER C. H., FEDORS N., FLORA N. J., BROWN H., HAMILTON K., SCHAEFFER C.D., *Synthesis and reactivity in inorganic and metal-organic chemistry*, J. The Existence of Pure-Phase Transition Metal Hydroxyl Apatites, 2004, 34, 1835–1842.
- [22] ZHAOGA G., XIAA L., WENA G., SONGA L., WANGA X., WUB K., *Microstructure and properties of plasma-sprayed bio-coatings on a low-modulus titanium alloy from milled Ha/Ti powders*, J. Surface and Coatings Technology, 2012, 206(23), 4711–4719.
- [23] ZASIŃSKA K., PIĄTKOWSKA A., *Ocena zużycia ściernego stopu Ti13Nb13Zr implantowanego jonami azotu, przeznaczonego na element trące w endoprotezach ortopedycznych*, J. Tribologia: Tarcie, Zużycie, Smarowanie, 2015, 6, 175–186.
- [24] ZEMTSOVA E.G., OREHOV E.V., ARBENIN A.Y. et al., *Creating nanocoating different morphology titanium dioxide on titanium matrix for bone implant*, J. Materials Physics and Mechanics, 2016, 29, 138–144.